

Vapor–Liquid Equilibrium Measurements of MTBE and TAME with Toluene

Daniel G. Vorenberg, J. David Raal, and Deresh Ramjugernath*

Thermodynamics Research Unit, School of Chemical Engineering, Howard College Campus, University of KwaZulu-Natal, Durban 4001, South Africa

This paper presents binary vapor–liquid equilibria (VLE) for the ether–aromatic systems including 2-methoxy-2-methylbutane (TAME) and 2-methoxy-2-methylpropane (MTBE) with toluene. The data sets were measured using a dynamic experimental method over a temperature range from (308 to 323) K. The isothermal data were correlated using several liquid-phase excess Gibbs energy models including NRTL, UNIQUAC, and the Wilson model, with the respective model parameters fitted using the Marquardt optimization algorithm. Infinite dilution activity coefficients in the oxygenate-depleted region are reported. The isothermal VLE data are shown to be thermodynamically consistent.

Introduction

Because of global environmental concerns over the current stock of oxygenate additives used for octane enhancement in gasoline blends, thermodynamic data are required by the petroleum industry for new and currently used additives. The resulting thermophysical data are important in process engineering design, gasoline blending, and the prediction of the environmental fate of oxygenate additives. In this work, isothermal vapor–liquid equilibrium (VLE) data were measured in a computer-controlled dynamic still for two ether–toluene systems. The ethers investigated were 2-methoxy-2-methylpropane (methyl tertiary-butyl ether, MTBE) and 2-methoxy-2-methylbutane (tertiary amyl methyl ether, TAME). This is in response to a call from worldwide environmental agencies, the petroleum industry, and other concerned organizations¹ to develop a set of recommended values for ether oxygenates. Although the slow phasing out of MTBE on a regional scale has begun, thermodynamic data for this chemical and its behavior in mixtures is still relevant as a benchmarking tool. The data measured in this work allows the comparison of MTBE with possible substitute chemicals in order to ascertain the relative antiknock, octane-enhancing, clean-burning capabilities of the replacement oxygenates.

P – x – y data were collected for MTBE + toluene at (308.15, 318.15, and 323.15) K, adding three new isothermal data sets to the single isothermal set currently available in the literature at 333.15 K². Moreover, P – x – y data at a temperature of 318.15 K were measured for the TAME + toluene system, enabling a direct comparison of the VLE behavior of the two ether + toluene systems at this temperature.

Experimental Section

Materials. All chemicals used in this work were purchased from Riedel-de-Haën. Although the minimum chemical purity guaranteed by the supplier for TAME was relatively low, gas chromatographic analysis of this reagent and the other reagents failed to show any significant

Table 1. Refractive Indices and Reagent Purities

reagent	refractive index (293.15 K)		minimum purity (%) ^b
	experimental	literature ^a	
MTBE	1.3698	1.3690	99.8
TAME	1.3862	1.3855	97.0
toluene	1.4965	1.4961	99.8

^a Reference 3. ^b As stated by the supplier.

Table 2. Vapor-Pressure Measurements for TAME and Comparison with Predictive Correlations

$P_{\text{measd}}/\text{kPa}$	$P_{\text{calcd}}/\text{kPa}$			T/K	$ \Delta P /\text{kPa}$		
	this work	ref 4	ref 5		this work	ref 4	ref 5
10.00	10.00	9.98	10.00	298.02	0.00	0.02	0.00
15.00	15.00	15.00	15.00	306.98	0.00	0.00	0.00
25.00	25.00	25.02	24.99	319.20	0.00	0.02	0.01
35.00	34.99	35.03	34.98	327.90	0.01	0.03	0.02
45.00	45.00	45.03	44.99	334.78	0.00	0.03	0.01
55.00	55.01	55.01	54.99	340.52	0.01	0.01	0.01
65.00	65.01	64.99	65.00	345.48	0.01	0.01	0.00
75.00	74.98	74.92	74.97	349.85	0.02	0.08	0.03
85.00	85.01	84.92	85.03	353.81	0.01	0.08	0.03
90.00	89.99	89.99	90.02	355.64	0.01	0.12	0.02

^a $|\Delta P| = |P_{\text{measd}} - P_{\text{calcd}}|$.

impurities. After a comparison of the measured refractive indices of the reagents with literature values, shown in Table 1, as well as a comparison of measured vapor-pressure points with literature values (Table 2), it was decided to use the reagents without further purification.

Measured vapor-pressure data for TAME from this work were correlated to a four-parameter equation (eq 1) as used by Reid et al.,⁶ and compared with predicted vapor pressures, as calculated using the three-parameter Antoine equations found in the DDB⁴ and in the work of Antosik and Sandler.⁵ This is shown in Table 2. The critical properties were obtained from the DDB.⁴

$$\ln\left(\frac{P^{\text{sat}}}{P_c}\right) = (1-x)^{-1}[VP_1x + VP_2x^{1.5} + VP_3x^3 + VP_4x^6] \quad (1)$$

* Corresponding author. E-mail: ramjager@ukzn.ac.za.

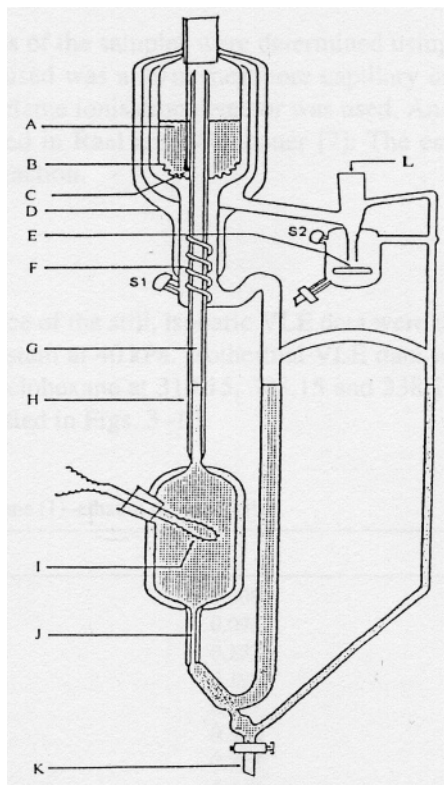


Figure 1. Schematic diagram of VLE equilibrium still: A, stainless steel wire mesh packing; B, drain holes; C, Pt-100 sensor; D, vacuum jacket; E, magnetic stirrer; F, stainless steel mixing spiral; G, insulated Cottrell pump; H, vacuum jacket; I, internal heater; J, capillary tube; K, drain valve; L, condenser attachment position; S1, liquid sampling point; S2, vapor sampling point.

where $x = 1 - T/T_c$, (T/K); $T_c = 536.3$ K; $P_c = 31.91$ bar; $VP_1 = -7.8714$; $VP_2 = 2.4416$; $VP_3 = -5.1738$; and $VP_4 = 2.9644$

Apparatus and Procedure. The apparatus consists of a dynamic VLE still (Figure 1), as modified by Raal⁷, a Sensotech Super TJE pressure transducer, a Hewlett-Packard (HP) model 34401 multimeter, a differential mercury manometer, a computer, two solenoid valves, a vacuum pump, two ballast flasks, a dc supply for motors driving magnetic stirrers in the vapor sampling chamber and boiling chamber, and two ac voltage regulators for the internal and external heaters. The computer control of the VLE measurement system has been discussed elsewhere⁸.

The boiling chamber is charged with the liquid sample, and the external heater is powered until initial signs of boiling begin to occur. The internal cartridge is then activated, forcing the vapor-liquid mixture upward through the Cottrell tube. The latter is vacuum jacketed to eliminate any heat transfer from the superheated mixture to the packed equilibrium chamber. The mixture then enters the equilibrium chamber where it flows over the packing, which consists of 3-mm stainless steel mesh cylinders, onto a Pt-100 temperature sensor that is located near the exit from the packed section. Equilibrium liquid exits through small drain holes at the bottom of the equilibrium chamber, flowing over a stainless steel mixing spiral to the liquid sampling trap, the overflow of which leads back to the boiling chamber. The disengaged vapor moves upward around the equilibrium chamber, thermally insulating the latter. The vapor flows through the insulated tubing to the condenser where it condenses into a condensate trap. The overflow from the condensate trap spills into a standpipe leg that feeds the bottom of the boiling chamber.

Table 3. Gas Chromatograph Settings for VLE Measurement

GC make	Hewlett-Packard
GC type	5890 series II
detector type	TCD
column type	packed (Poropak Q)
column length/m	2
column outer diameter/in.	1/8
injection temperature/ $^{\circ}$ C	270
column temperature/ $^{\circ}$ C	200
detector temperature/ $^{\circ}$ C	250
carrier gas flow rate/ $\text{mL}\cdot\text{min}^{-1}$	30

Temperature and Pressure Measurement and Control. An HP five and a half digit multimeter was used to display the resistance measured by the Pt-100 sensor. The pressure was monitored with a pressure transducer. The accuracies of the respective temperature and pressure measurements are estimated to be ± 0.02 K and ± 0.03 kPa. Pressure control in the still was observed to be within 0.01 kPa. The temperature control exhibited by the computer control strategy varied between 0.01 K and 0.05 K about the setpoint depending on the composition region of the charge. The control strategy was based upon the pulse-width modulation of two solenoid valves fixed to the vacuum and atmospheric lines.

Composition Analysis. The equilibrium phase samples were analyzed using an HP 5890 series II model gas chromatograph (GC), which was equipped with a thermal conductivity detector (TCD) and a Poropak Q packed column. The compositional analysis was based on the GC area ratio method as discussed by Raal and Mühlbauer.⁷ The estimated uncertainty in the vapor and liquid samples is believed to be ± 0.002 mole fraction. The GC settings used in this work are presented in Table 3.

Results and Discussion

The four measured P - T - x - y data sets were regressed according to the γ/φ formulation. Three activity coefficient models, including the Wilson,⁹ NRTL,¹⁰ and UNIQUAC,¹¹ were fit using the Marquardt¹² algorithm, which was compiled to minimize the pressure residual. Nonideality in the vapor phase was accounted for using the second virial coefficient correlation of Tsionopoulos and Dymond.¹³ Ignoring vapor-phase nonidealities would have induced a maximum relative error of 3.5% in the low-pressure systems investigated in this work.

As illustrated in Figures 2 and 3, all systems measured exhibited nearly ideal vapor-liquid equilibria and no azeo-

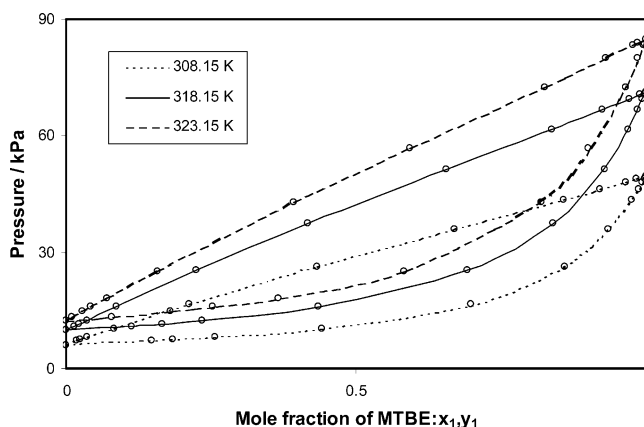


Figure 2. Experimental P - x - y data and parametrized Wilson activity coefficient fitted curves for MTBE (1) + toluene (2) at (308.15, 318.15, and 323.15) K. (Circles indicate experimental points.)

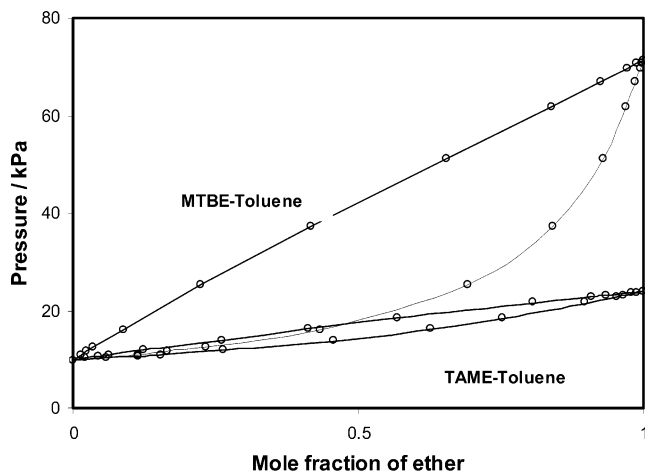


Figure 3. Experimental P - x - y data and parametrized Wilson activity coefficient model fitted curves for MTBE and TAME in toluene at 318.15 K. (Circles indicate experimental points.)

Table 4. Vapor-Liquid Equilibrium Measurements for MTBE (1) + Toluene (2) at (308.15, 318.15, and 323.15) K

MTBE (1) + toluene (2)								
308.15 K			318.15 K			323.15 K		
x_1	y_1	P/kPa	x_1	y_1	P/kPa	x_1	y_1	P/kPa
0.000	0.000	6.18	0.000	0.000	9.88	0.000	0.000	12.28
0.018	0.147	7.12	0.015	0.114	10.99	0.011	0.080	13.20
0.024	0.185	7.44	0.023	0.165	11.57	0.028	0.181	14.65
0.037	0.251	8.04	0.036	0.234	12.46	0.043	0.254	15.89
0.082	0.434	10.32	0.088	0.435	16.05	0.071	0.366	18.18
0.212	0.698	16.50	0.224	0.693	25.27	0.158	0.584	25.19
0.433	0.86	26.28	0.417	0.841	37.36	0.393	0.820	42.78
0.671	0.936	36.06	0.656	0.929	51.24	0.594	0.901	56.76
0.859	0.977	43.60	0.839	0.970	61.73	0.826	0.966	72.55
0.921	0.988	46.14	0.926	0.987	66.87	0.931	0.987	79.92
0.966	0.995	48.05	0.971	0.995	69.61	0.977	0.996	83.21
0.984	0.997	48.83	0.989	0.998	70.74	0.985	0.997	83.80
1.000	1.000	49.48	1.000	1.000	71.41	1.000	1.000	84.91

Table 5. Vapor-Liquid Equilibrium Measurements for TAME (1) + Toluene (2) at 318.15 K

TAME (1) + Toluene (2)		
x_1	y_1	P/kPa
0.000	0.000	12.28
0.011	0.080	13.20
0.028	0.181	14.65
0.043	0.254	15.89
0.071	0.366	18.18
0.158	0.584	25.19
0.393	0.820	42.78
0.594	0.901	56.76
0.826	0.966	72.55
0.931	0.987	79.92
0.977	0.996	83.21
0.985	0.997	83.80
1.000	1.000	84.91

trope were observed in the temperature range investigated. The measured VLE data points are presented in Tables 4 and 5. Activity coefficient parameters and mean residuals for both pressure and vapor mole fraction are presented in Table 6.

Thermodynamic Consistency. The thermodynamic consistency of the isothermal data was checked using the point-to-point test of van Ness et al.,¹⁴ which advocates that the thermodynamic consistency of the data can be judged by the difference between the predicted and experimental vapor compositions. Danner and Gess¹⁵ stipulate that the absolute deviation between the calculated and experimental vapor-phase mole fractions must be less than 0.01.

Table 6. Correlated Activity Coefficient Model Parameters and Mean Pressure and Vapor Mole Fraction Residuals

activity coefficient model	binary VLE system			
	MTBE (1) + toluene (2)		TAME (1) + toluene (2)	
	$T = 308.15$ K	318.15 K	323.15 K	318.15 K
Wilson				
$(\lambda_{12} - \lambda_{11})/\text{J}\cdot\text{mol}^{-1}$	-373.1	-222.5	-209.0	-1496.6
$(\lambda_{12} - \lambda_{22})/\text{J}\cdot\text{mol}^{-1}$	999.4	847.3	818.2	2268.5
average Δy_1	0.002	0.001	0.002	0.005
average $\Delta P/\text{kPa}$	0.04	0.03	0.01	0.04
UNIQUAC				
$(u_{12} - u_{11})/\text{J}\cdot\text{mol}^{-1}$	1566.0	1483.8	1500.5	1962.7
$(u_{12} - u_{22})/\text{J}\cdot\text{mol}^{-1}$	-1211.3	-1166.6	-1185.3	-1456.6
average Δy_1	0.002	0.001	0.002	0.005
average $\Delta P/\text{kPa}$	0.04	0.03	0.02	0.04
NRTL				
$(g_{12} - g_{11})/\text{J}\cdot\text{mol}^{-1}$	1761.2	1577.8	1514.6	1521.0
$(g_{12} - g_{22})/\text{J}\cdot\text{mol}^{-1}$	-1019.7	-855.7	-856.6	-994.1
α	0.3	0.3	0.3	0.3
average Δy_1	0.001	0.001	0.001	0.005
average $\Delta P/\text{kPa}$	0.04	0.04	0.03	0.05

According to these criteria, the mean vapor fraction residuals presented in Table 6 indicate that all of the experimental isothermal data sets are thermodynamically consistent.

Although small additions of MTBE have a very small effect on the total equilibrium pressure¹⁶ and, consequently, on the Reid vapor pressure, TAME is expected to contribute less to the total gasoline blend pressure judging from the P - x - y curves in Figure 3.

Infinite Dilution Activity Coefficients. According to Pividal et al.,¹⁷ for systems at low to moderate pressures, the infinite dilution activity coefficient is related to the partial derivative of the system pressure with respect to liquid mole fraction by the following equation:

$$\gamma_i^{\infty} = \epsilon_i \frac{P_j^{\text{sat}}}{P_i^{\text{sat}}} \left(1 + \frac{\beta_j}{P_j^{\text{sat}}} \left[\frac{\partial P}{\partial x_1} \right]_{T, x_1 \rightarrow 0} \right) \quad (2)$$

where

$$\epsilon_i^{\infty} = \exp \left(\frac{(B_{ii} - V_i^L)(P_j^{\text{sat}} - P_i^{\text{sat}}) + \delta_{ij} P_j^{\text{sat}}}{RT} \right)$$

$$\beta_j = 1 + P_j^{\text{sat}} \left(\frac{B_{ij} - V_j^L}{RT} \right)$$

$$\delta_{ij} = 2B_{ij} - B_{ii} - B_{jj}$$

The accuracy of the infinite dilution activity coefficient is dependent on the accuracy of the pressure-composition derivative. The partial derivative dependency of pressure on liquid composition was generated by fitting the pressure data in the dilute region to eq 3. This technique has been previously used by Sandler and others.^{17,18} A linear equation was regressed owing to the linear nature of the measured P - x data curves,

$$P = a + bx_1 \quad (3)$$

The pressure-liquid mole fraction derivative is thus equal to b , the gradient of eq 3.

Only the infinite dilution coefficients of oxygenate in toluene were regressed because the oxygenate dilute region is of greater significance in the environmental assessment

Table 7. Limiting Activity Coefficients of the Ethers, MTBE and TAME, in Toluene, Pure Ether Vapor Pressures, and Ether Henry's Constants in Toluene

oxygenate property	T/K		
	308.15	318.15	323.15
infinite dilution activity coefficient, γ_1^∞			
MTBE (1) + toluene (2)	1.18	1.15	1.14
TAME (1) + toluene (2)		1.13	
vapor pressure, P_i^{sat} /kPa			
MTBE	49.48	71.41	84.91
TAME		23.99	
Henry's constant in toluene, \hat{H}_1 /kPa			
MTBE (1) + toluene (2)	58.37	82.12	96.80
TAME (1) + toluene (2)		27.11	

of gasoline oxygenate behavior. The limiting activity coefficients, saturated vapor pressure, and Henry's constants for the oxygenate ethers in toluene are presented in Table 7.

Conclusions

TAME, when compared with MTBE, has a lower Henry's constant, which reflects TAME's reduced tendency to equilibrate into air from an aromatic mixture. Both ether-aromatic systems display nearly ideal behavior containing no azeotropes. The binary systems were fit satisfactorily by all of the activity coefficient models employed (Wilson, NRTL, and UNIQUAC), with the Wilson model showing a marginally superior fit.

Literature Cited

- (1) Marsh, K. N.; Niamskul, P.; Gmehling, J.; Bölts, R. Review of Thermophysical Property Measurements on Mixtures Containing MTBE, TAME, and Other Ethers with Non-polar Solvents. *Fluid Phase Equilib.* **1999**, *156*, 207–227.
- (2) Plura, J.; Matous J.; Novak, J. P.; Sobr, Vapor-Liquid Equilibrium in the Methyl tert-Butyl Ether – n-Hexane and Methyl tert-Butyl Ether – Toluene Systems. *Collect. Czech. Chem. Commun.* **1979**, *44*, 3627–3631.
- (3) POC. *Properties of Organic Compounds*, Web version 6.0; Chapman & Hall/CRC Press: copyright 1982–2002; www.chemnetbase.com/Scripts/pocweb.exe.
- (4) Dortmund Data Bank Software, purchased 1998.
- (5) Antosik, M.; Sandler, S. I. Vapor–Liquid Equilibria of Hydrocarbons and tert-Amyl Methyl Ether. *J. Chem. Eng. Data* **1994**, *39*, 584–587.
- (6) Reid, R. C.; Prausnitz, J. M.; Poling B. E. *The Properties of Gases and Liquids*; 4th ed.; McGraw-Hill: New York, 1987; Appendix A.
- (7) Raal, J. D.; Mühlbauer, A. L. *Phase Equilibria: Measurement and Computation*; Taylor & Francis: Washington, DC, 1998; Chapters 2 and 4.
- (8) Joseph, M. A.; Raal, J. D.; Ramjugernath, D. Phase Equilibrium Properties of Binary Systems with Diacetyl from a Computer Controlled Vapour-Liquid Equilibrium Still. *Fluid Phase Equilib.* **2001**, *182*, 157–176.
- (9) Wilson, G. M. Vapor–Liquid Equilibrium. XI. A New Expression for the Excess Free Energy of Mixing. *J. Am. Chem. Soc.* **1964**, *86*, 127–130.
- (10) Renon, H.; Prausnitz, J. M. Local Compositions in Thermodynamic Excess Functions for Liquid Mixtures. *AIChE J.* **1968**, *14*, 135–144.
- (11) Abrams, D. S.; Prausnitz, J. M. Statistical Thermodynamics of Liquid Mixtures: A New Expression for the Excess Gibbs Energy of Partly or Completely Miscible Systems. *AIChE J.* **1975**, *21*, 116–128.
- (12) Marquardt, D. W.; An Algorithm for Least-squares Estimation of Nonlinear Parameters. *J. Soc. Ind. Appl. Math.* **1963**, *11*, 431–441.
- (13) Tsonopoulos, C.; Dymond, J. H. Second Virial Coefficients of Normal Alkanes, Linear 1-Alkanols (and Water), Alkyl Ethers, and their Mixtures. *Fluid Phase Equilib.* **1997**, *133*, 11–34.
- (14) van Ness, H. C.; Byers, M.; Gibbs, R. E. Vapor-Liquid Equilibrium: Part I. An Appraisal of Data Reduction Methods. *AIChE J.* **1973**, *19*, 238–251.
- (15) Danner, R. P.; Gess, M. A. A Data Base Standard for the Evaluation of Vapor-Liquid-Equilibrium Models. *Fluid Phase Equilib.* **1990**, *56*, 285–301.
- (16) Bennett, A.; Lamm, S.; Orbey, H.; Sandler, S. I. Vapor–Liquid Equilibria of Hydrocarbons and Fuel Oxygenates. 2. *J. Chem. Eng. Data* **1993**, *38*, 263–269.
- (17) Pividal, K. A.; Birtigh, A.; Sandler, S. I. Infinite Dilution Activity Coefficients for Oxygenate Systems Determined Using a Differential Static Cell. *J. Chem. Eng. Data* **1992**, *37*, 484–487.
- (18) Wright, D. A.; Sandler, S. I.; DeVoll, D. Infinite Dilution Activity Coefficients and Solubilities of Halogenated Hydrocarbons in Water at Ambient Temperatures. *Environ. Sci. Technol.* **1992**, *26*, 1828–1831.

Received for review April 2, 2004. Accepted October 4, 2004. We acknowledge the financial support given to this work by Sasol (Pty) Ltd. and THRIP.

JE049867T